Excess Dynamic Viscosity and Excess Volume of *N*-Butylamine + 1-Alkanol Mixtures at Moderately High Pressures

Dimitrios Papaioannou, Michael Bridakis, and Constantinos G. Panayiotou*

Department of Chemical Engineering, University of Thessaloniki, 54006 Thessaloniki, Greece

Experimental measurements are reported for the dynamic viscosity and the density of the four binary mixtures of *n*-butylamine with methanol, ethanol, 1-propanol, and 1-butanol. The measurements were conducted at 25 °C and in a pressure range from atmospheric to 720 bar for the dynamic viscosity and from atmospheric to 340 bar for the density. The self-centering falling body viscometer used is described in detail. Calculated excess volumes, compressibilities, and excess viscosities are also reported. The systems studied, besides self-association, exhibit very strong cross-association due to the strong hydrogen bonding between the hydroxyl and the amine groups. As a consequence of this strong intermolecular association all four systems studied exhibit relatively large negative excess volumes while the first two systems with the lower alkanols exhibit pronounced maxima in the excess viscosity.

Introduction

Over the last few years we have been conducting a systematic study of the basic thermophysical properties of representative hydrogen-bonded systems, primarily liquids, such as volumetric properties, phase equilibria, heats of mixing, interfacial properties, and dynamic viscosities. The behavior of this class of systems deviates remarkably from ideal solution behavior, and such systematic experimental work is needed not only for a rational process equipment or process plant design but also for the advancement of theoretical developments through an understanding of the intermolecular forces–solution structure–property relationships.

The focus in this work is on the effect of pressure on the density and dynamic viscosity of four binary mixtures of *n*-butylamine with the series of 1-alkanols from methanol to 1-butanol. Parallel measurements of the heats of mixing in these systems are showing that the hydroxyl–amine interaction is one of the strongest hydrogen bonds. It would then be interesting to see how hydrogen bonding manifests itself at higher pressures. Although the pressures applied are not very high, we believe that some trends are rather clear. As we made clear in a recent work (*1*), a most useful quantity encountered when applying free-volume theories of viscosity is the limit of the ratio of viscosity over pressure as the pressure tends to zero. Systematic data on this limiting quantity are rather scarce in the literature. The experimental data reported in the present work are ideally suited for the evaluation of this quantity.

Experimental Section

Materials. All materials used are pro-analysis grades from Merck. Their purity was verified by gas–liquid chromatography and was better than 99.8 mol % for methanol, 99.5 mol % for ethanol, 1-propanol, and 1-butanol, and 99.0 mol % for *n*-butylamine. The liquids were used as received. Pure component properties are shown in Table I. The mixtures were prepared by mass with a precision of ±0.0001 g.

* To whom correspondence should be addressed.

Table I. Pure Component Properties at 298.15 K

	ρ/(Kg·m^{-3})		η/(mPa·s)	
liquid	measd	lit.	measd	lit.
methanol	786.7	787.0[a]	0.546	0.546[a]
ethanol	785.1	785.2[b]	1.083	1.081[b]
1-propanol	799.6	800.0[b]	1.968	1.942[b]
1-butanol	805.9	806.0[c]	2.578	2.600[d]
n-butylamine	732.2	733.1[e]	0.468	0.470[f]

[a] Referrence 11. [b] Reference 12. [c] Reference 13. [d] Reference 14. [e] Reference 15. [f] Reference 16.

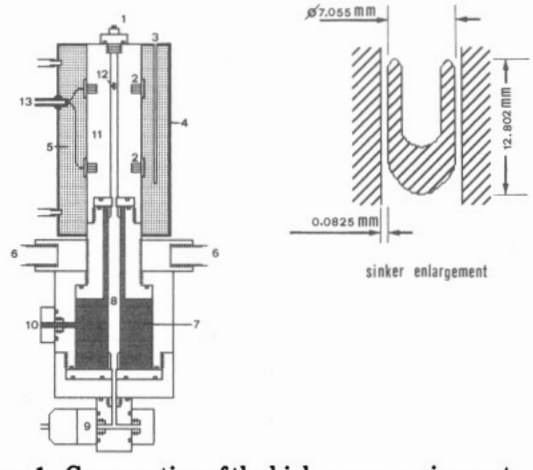

Figure 1. Cross section of the high-pressure viscometer with an enlargement of the falling body (sinker): (1) crub screw plug; (2) triggering coils; (3) housing of the temperature sensor; (4) thermostatic jacket; (5) circulating thermostatic fluid; (6) bearing bars; (7) hydraulic-compression fluid; (8) flexible Teflon tube filled with the studied fluid; (9) pressure transducer; (10) connection to the dead-weight tester; (11) viscometer tube; (12) sinker; (13) exit of electric cables.

Precautions were taken in order to minimize evaporation losses during storage and preparation of the solutions.

Density. The liquid densities, ρ, at atmospheric pressures were measured with a vibrating-tube densitometer (Anton Paar Model DMA 60/602). Bidistilled water and air were used as calibrating substances. The densities at higher

0021-9568/93/1738-0370$04.00/0

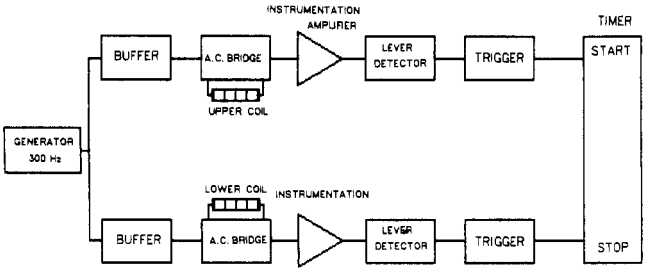

Figure 2. Schematic diagram of the electronic connections of the high-pressure viscometer.

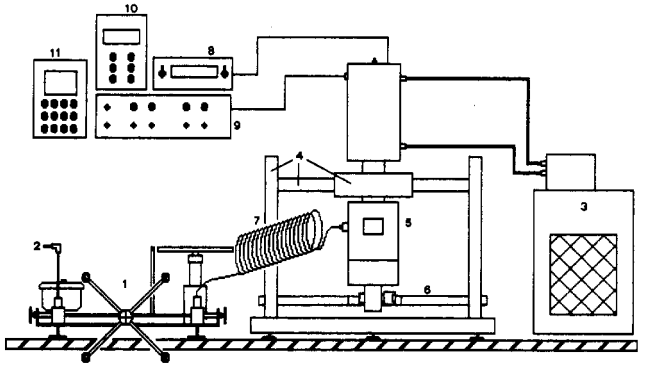

Figure 3. Experimental setup for the measurement of viscosity at high pressures. (1) dead-weight tester; (2) exit to densitometer; (3) circulating ultrathermostat; (4) bearing bars; (5) viscometer; (6) bar for vertical positioning; (7) flexible stainless steel tube; (8) pressure indicator; (9) signal generator and amplifier; (10) chronometer; (11) palmograph; (12) viscometer base adjustable to exactly horizontal position.

pressures were measured with equipment described earlier (*2*). It consisted of a high-pressure density cell (Anton Paar Model DMA 512), a home-made compression cell equipped with a pressure transducer (Druck Model PDCR 610), and a dead-weight tester (Metronex Model MTU600). The compression cell consisted of an outer stainless steel cylinder, along the axis of which was located a thin-wall Teflon tube containing the sample. Outside the Teflon tube was the compression fluid—a commercial hydraulic fluid. The equipment was calibrated with experimental high-pressure densities of water (*3*) and methanol (*4*). No hysteresis was observed in the density measurements by increasing and then decreasing the external pressure. The temperature in the measuring cells was regulated to 25.00 ± 0.01 °C through a Haake ultrathermostat and measured by a (Systemteknik Model S1220) precision digital thermometer, equipped with a specially designed sensor. The estimated error in the density at atmospheric pressure is ±5 × 10^{-6} g·cm^{-3} while the corresponding error in the density at higher pressures is ±1 × 10^{-4} g·cm^{-3}.

Viscosity. For the measurement of the dynamic viscosity at high pressures a self-centering falling body viscometer (*5–8*) has been constructed in which a sinker falls axially down the center of a vertical circular tube containing the liquid whose viscosity is to be measured. The primary quantity which is measured is the terminal velocity of the sinker. The terminal velocity, u, of a cylindrical body falling axially down a closed vertical tube containing a liquid at constant temperature, T, and pressure, P, can be obtained by solving the equations governing the motion. When laminar flow prevails, the above-mentioned equations when solved give (*5*)

$$u = -\frac{m_S g(1-\rho_L/\rho_S)}{2\pi L_S \eta}\left\{\ln\left(\frac{r}{r_S}\right) - \frac{(r^2-r_S^2)}{(r^2+r_S^2)}\right\} \quad (1)$$

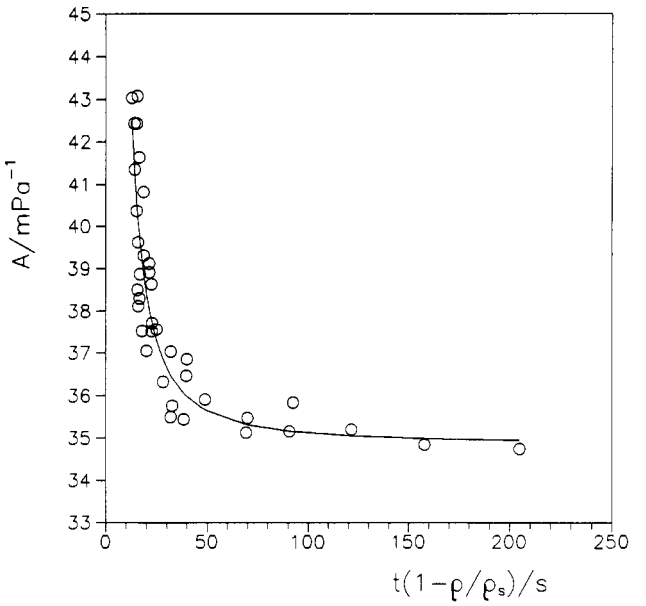

Figure 4. Calibration curve for the high-pressure viscometer constant A.

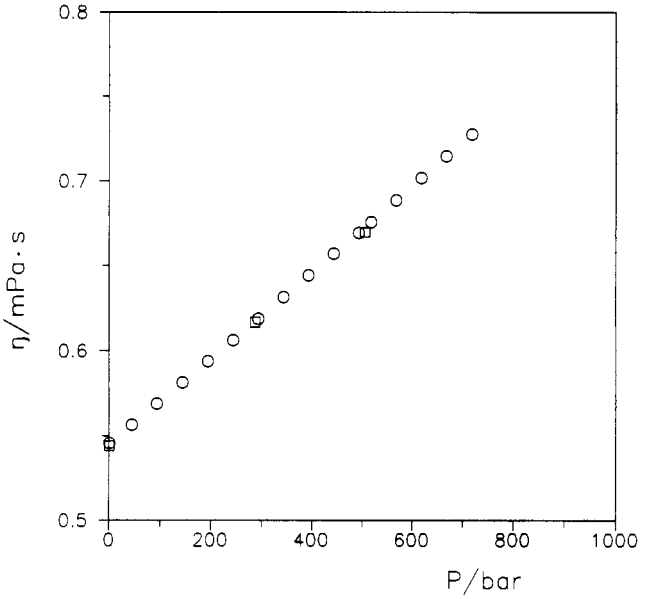

Figure 5. Pressure dependence of the dynamic viscosity of methanol at 298.15 K: □, experimental data from Isdale et al. (*8*); ○, this work.

where m_S, ρ_S, L_S, and r_S are the mass, the density, the length, and the radius of the sinker, respectively. ρ_L and η are the density and the shear viscosity of the liquid, respectively, while r is the internal radius of the tube. In the case of an instrument with a tube and sinker of the same material, eq 1 is reduced to (*5*)

$$\eta = \frac{t(1-\rho_L/\rho_S)}{A[1+2\alpha(T-T_r)][1-(2/3)\beta(P-P_r)]} \quad (2)$$

where t is the falling time of the sinker, T_r is the reference temperature (taken, here, to be 25 °C), P_r is the reference pressure (taken to be 1.013 bar), α is the linear coefficient of thermal expansion of the tube and sinker, and A is the viscometer constant. Although eqs 1 and 2 would allow the viscometer to be used for absolute measurements, the difficulties associated with the precise determination of the viscometer constant A prevent it in practice. A is strongly

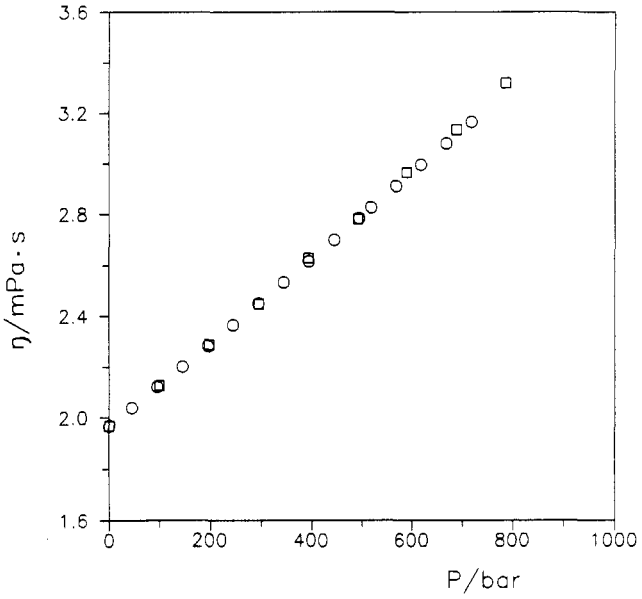

Figure 6. Pressure dependence of the dynamic viscosity of 1-propanol at 298.15 K: □, experimental data from Tanaka et al. (*9*); ○, this work.

dependent on the difference between the radii of the tube and sinker. $r - r_S$ must be kept small so that the viscous forces incurred at the entry and exit of the annulus are small compared with the forces acting within the annulus. It follows then that small errors in the measurement of the radii can produce large errors in the calculated value of A. In practice therefore the viscometer constant is calculated from measurements at atmospheric pressure in liquids of accurately known viscosity. A is theoretically independent of temperature, pressure, and viscosity for laminar coaxial flow.

The main body of the viscometer is schematically shown in Figure 1. It consists of a vertical tube, a pair of triggering coils, the sinker, and the pressure-transmitting device. The nonmagnetic stainless steel tube is 200 mm in length. Its internal and external diameters are 7.220 and 50.00 mm, respectively. The sinker is made out of a magnetic material and has the shape of a hollow cylinder with a hemispherical nose at the bottom end. An enlargement of the sinker is shown on the right in Figure 1. The edge of the open end of the cylinder was radiused so that no sharp corners were formed. After external surface was finished, the sinker was covered electrolytically with pure Ni. After these treatments the sinker was 12.803 mm in length and 7.055 mm in diameter, leaving thus an annulus of 0.0825 mm between the tube and the sinker. The diameters of both the tube and sinker are constants to within ±0.005 mm and deviate from circularity by less than 0.005 mm.

The working length of the viscometer tube is the distance between the two triggering coils, permanently wound outside the tube. A 44-swg insulated copper wire with a resistance of 80 Ω is used in the coils with 550 turns in each. The pair of coils are connected to form an ac bridge circuit which is initially balanced. The bridge circuit is shown in Figure 2. When the sinker passes through the coils, the inductance of each coil increases in turn and the bridge is unbalanced. The

Table II. Experimental Densities, Excess Volumes, and Compressibilities β for the System Methanol (1) + *n*-Butylamine (2) at 298.15 K

P/bar	ρ/ (g·cm^{-3})	V^E/ (cm^3·mol^{-1})	$10^4\beta_T$/bar^{-1}	P/bar	ρ/ (g·cm^{-3})	V^E/ (cm^3·mol^{-1})	$10^4\beta_T$/bar^{-1}	P/bar	ρ/ (g·cm^{-3})	V^E/ (cm^3·mol^{-1})	$10^4\beta_T$/bar^{-1}
					$x_1 = 0.000$						
1.0	0.7322	0.00	1.055	119.7	0.7409	0.00	0.952	289.2	0.7523	0.00	0.846
20.0	0.7336	0.00	1.037	159.6	0.7437	0.00	0.923	339.0	0.7554	0.00	0.823
59.9	0.7366	0.00	1.000	199.5	0.7464	0.00	0.896				
79.8	0.7381	0.00	0.983	239.3	0.7490	0.00	0.873				
					$x_1 = 0.1968$						
1.0	0.7450	−0.929	1.010	119.7	0.7535	−0.863	0.911	289.2	0..7645	−0.783	0.811
20.0	0.7464	−0.918	0.992	159.6	0.7562	−0.842	0.884	339.0	0.7676	−0.762	0.789
59.9	0.7493	−0.895	0.958	199.5	0.7588	−0.823	0.859				
79.8	0.7507	−0.884	0.942	239.3	0.7614	−0.805	0.837				
					$x_1 = 0.4023$						
1.0	0.7596	−1.574	0.972	119.7	0.7680	−1.464	0.882	289.2	0.7789	−1.338	0.790
20.0	0.7610	−1.555	0.956	159.6	0.7707	−1.432	0.857	339.0	0.7820	−1.307	0.770
59.9	0.7639	−1.517	0.924	199.5	0.7733	−1.401	0.834				
79.8	0.7653	−1.499	0.909	239.3	0.7758	−1.372	0.813				
					$x_1 = 0.4983$						
1.0	0.7661	−1.676	0.967	119.7	0.7746	−1.562	0.881	289.2	0.7856	−1.436	0.794
20.0	0.7675	−1.657	0.951	159.6	0.7772	−1.529	0.857	339.0	0.7887	−1.406	0.775
59.9	0.7704	−1.617	0.921	199.5	0.7799	−1.498	0.835				
79.8	0.7718	−1.598	0.907	239.3	0.7825	−1.469	0.816				
					$x_1 = 0.5998$						
1.0	0.7724	−1.628	0.983	119.7	0.7809	−1.520	0.881	289.2	0.7919	−1.383	0.772
20.0	0.7738	−1.610	0.965	159.6	0.7837	−1.486	0.852	339.0	0.7949	−1.345	0.746
59.9	0.7767	−1.573	0.929	199.5	0.7863	−1.454	0.825				
79.8	0.7782	−1.555	0.913	239.3	0.7889	−1.422	0.800				
					$x_1 = 0.7998$						
1.0	0.7819	−1.074	1.0220	119.7	0.7910	−0.996	0.9269	289.2	0.8028	−0.908	0.8239
20.0	0.7834	−1.061	1.0053	159.6	0.7939	−0.973	0.8995	339.0	0.8060	−0.887	0.7996
59.9	0.7865	−1.033	0.9722	199.5	0.7967	−0.951	0.8741				
79.8	0.7880	−1.020	0.9565	239.3	0.7994	−0.931	0.8507				
					$x_1 = 1.0000$						
1.0	0.7867	0.00	1.192	119.7	0.7973	0.00	1.069	289.2	0.8108	0.00	0.927
20.0	0.7884	0.00	1.170	159.6	0.8006	0.00	1.032	339.0	0.8145	0.00	0.891
59.9	0.7921	0.00	1.128	199.5	0.8039	0.00	0.998				
79.8	0.7938	0.00	1.108	239.3	0.8070	0.00	0.965				

Table III. Experimental Densities, Excess Volumes, and Compressibilities β for the System Ethanol (1) + n-Butylamine (2) at 298.15 K

P/bar	ρ/ (g·cm^{-3})	V^E/ (cm^3·mol^{-1})	$10^4\beta_T$/bar^{-1}	P/bar	ρ/ (g·cm^{-3})	V^E/ (cm^3·mol^{-1})	$10^4\beta_T$/bar^{-1}	P/bar	ρ/ (g·cm^{-3})	V^E/ (cm^3·mol^{-1})	$10^4\beta_T$/bar^{-1}
					x_1 = 0.1973						
1.0	0.7454	−0.800	1.013	119.7	0.7539	−0.747	0.917	289.2	0.7651	−0.687	0.820
20.0	0.7468	−0.791	0.996	159.6	0.7567	−0.731	0.890	339.0	0.7682	−0.673	0.799
59.9	0.7497	−0.772	0.962	199.5	0.7593	−0.716	0.866				
79.8	0.7511	−0.763	0.946	239.3	0.7619	−0.703	0.884				
					x_1 = 0.4013						
1.0	0.7580	−1.197	0.971	119.7	0.7664	−1.104	0.886	289.2	0.7774	−1.007	0.802
20.0	0.7594	−1.180	0.955	159.6	0.7691	−1.077	0.863	339.0	0.7805	−0.986	0.784
59.9	0.7623	−1.148	0.926	199.5	0.7717	−1.053	0.842				
79.8	0.7637	−1.132	0.912	239.3	0.7743	−1.032	0.823				
					x_1 = 0.4993						
1.0	0.7642	−1.288	0.978	119.7	0.7727	−1.200	0.887	289.2	0.7837	−1.100	0.793
20.0	0.7656	−1.273	0.962	159.6	0.7754	−1.174	0.862	339.0	0.7868	−1.075	0.773
59.9	0.7685	−1.243	0.930	199.5	0.7780	−1.150	0.838				
79.8	0.7699	−1.228	0.915	239.3	0.7806	−1.127	0.817				
					x_1 = 0.6102						
1.0	0.7707	−1.271	0.997	119.7	0.7792	−1.185	0.887	289.2	0.7904	−1.087	0.793
20.0	0.7721	−1.256	0.961	159.6	0.7820	−1.160	0.861	339.0	0.7935	−1.063	0.771
59.9	0.7750	−1.226	0.930	199.5	0.7846	−1.136	0.838				
79.8	0.7764	−1.212	0.915	239.3	0.7872	−1.113	0.817				
					x_1 = 0.7996						
1.0	0.7794	−0.864	1.005	119.7	0.7883	−0.806	0.910	289.2	0.7998	−0.739	0.809
20.0	0.7809	−0.854	0.988	159.6	0.7911	−0.788	0.883	339.0	0.8030	−0.722	0.785
59.9	0.7839	−0.834	0.955	199.5	0.7939	−0.772	0.858				
79.8	0.7854	−0.824	0.939	239.3	0.7966	−0.757	0.835				
					x_1 = 1.0000						
1.0	0.7852	0.00	1.080	119.7	0.7948	0.00	0.974	289.2	0.8072	0.00	0.855
20.0	0.7868	0.00	1.061	159.6	0.7978	0.00	0.943	339.0	0.8106	0.00	0.826
59.9	0.7901	0.00	1.024	199.5	0.8008	0.00	0.914				
79.8	0.7917	0.00	1.007	239.3	0.8037	0.00	0.886				

Table IV. Experimental Densities, Excess Volumes, and Compressibilities β for the System 1-Propanol (1) + n-Butylamine (2) at 298.15 K

P/bar	ρ/ (g·cm^{-3})	V^E/ (cm^3·mol^{-1})	$10^4\beta_T$/bar^{-1}	P/bar	ρ/ (g·cm^{-3})	V^E/ (cm^3·mol^{-1})	$10^4\beta_T$/bar^{-1}	P/bar	ρ/ (g·cm^{-3})	V^E/ (cm^3·mol^{-1})	$10^4\beta_T$/bar^{-1}
					x_1 = 0.2096						
1.0	0.7494	−0.755	0.991	119.7	0.7578	−0.701	0.899	289.2	0.7688	−0.642	0.807
20.0	0.7508	−0.746	0.975	159.6	0.7605	−0.686	0.874	339.0	0.7719	−0.628	0.787
59.9	0.7536	−0.727	0.942	199.5	0.7631	−0.671	0.851				
79.8	0.7551	−0.718	0.927	239.3	0.7657	−0.657	0.830				
					x_1 = 0.4001						
1.0	0.7645	−1.150	0.954	119.7	0.7727	−1.075	0.866	289.2	0.7835	−0.987	0.777
20.0	0.7658	−1.137	0.938	159.6	0.7754	−1.052	0.841	339.0	0.7865	−0.964	0.757
59.9	0.7687	−1.111	0.907	199.5	0.7780	−1.031	0.819				
79.8	0.7700	−1.099	0.893	239.3	0.7805	−1.011	0.799				
					x_1 = 0.4957						
1.0	0.7716	−1.222	0.943	119.7	0.7799	−1.150	0.862	289.2	0.7908	−1.075	0.782
20.0	0.7730	−1.209	0.928	159.6	0.7825	−1.130	0.840	339.0	0.7938	−1.058	0.764
59.9	0.7758	−1.184	0.900	199.5	0.7851	−1.111	0.820				
79.8	0.7772	−1.172	0.887	239.3	0.7877	−1.094	0.802				
					x_1 = 0.5980						
1.0	0.7787	−1.197	0.922	119.7	0.7869	−1.118	0.842	289.2	0.7976	−1.029	0.761
20.0	0.7801	−1.184	0.908	159.6	0.7895	−1.095	0.820	339.0	0.8006	−1.007	0.743
59.9	0.7829	−1.156	0.880	199.5	0.7921	−1.073	0.800				
79.8	0.7842	−1.143	0.866	239.3	0.7946	−1.052	0.781				
					x_1 = 0.7977						
1.0	0.7908	−0.829	0.930	119.7	0.7991	−0.782	0.844	289.2	0.8100	−0.721	0.752
20.0	0.7922	−0.821	0.915	159.6	0.8018	−0.768	0.819	339.0	0.8130	−0.704	0.731
59.9	0.7950	−0.805	0.885	199.5	0.8044	−0.753	0.796				
79.8	0.7964	−0.798	0.870	239.3	0.8069	−0.739	0.776				
					x_1 = 1.0000						
1.0	0.7996	0.00	0.942	119.7	0.8082	0.00	0.859	289.2	0.8194	0.00	0.771
20.0	0.8010	0.00	0.928	159.6	0.8109	0.00	0.836	339.0	0.8225	0.00	0.750
59.9	0.8039	0.00	0.899	199.5	0.8136	0.00	0.814				
79.8	0.8054	0.00	0.885	239.3	0.8162	0.00	0.794				

out of balance signals are properly modified and used to stimulate a trigger which starts and stops an electronic timer when the sinker passes through the first and second coils, respectively. The out of balance signals can be detected easily

Table V. Experimental Densities, Excess Volumes, and Compressibilities β for the System 1-Butanol (1) + n-Butylamine (2) at 298.15 K

P/bar	ρ/ (g·cm⁻³)	V^E/ (cm³·mol⁻¹)	$10^4\beta_T$/bar⁻¹	P/bar	ρ/ (g·cm⁻³)	V^E/ (cm³·mol⁻¹)	$10^4\beta_T$/bar⁻¹	P/bar	ρ/ (g·cm⁻³)	V^E/ (cm³·mol⁻¹)	$10^4\beta_T$/bar⁻¹
						x_1 = 0.2011					
1.0	0.7521	−0.786	0.970	119.7	0.7604	−0.728	0.893	289.2	0.7715	−0.690	0.821
20.0	0.7534	−0.775	0.956	159.6	0.7631	−0.715	0.872	339.0	0.7746	−0.687	0.807
59.9	0.7563	−0.754	0.929	199.5	0.7657	−0.704	0.854				
79.8	0.7578	−0.745	0.916	239.3	0.7683	−0.696	0.838				
						x_1 = 0.3957					
1.0	0.7689	−1.131	0.941	119.7	0.7771	−1.065	0.851	289.2	0.7877	−0.977	0.758
20.0	0.7703	−1.120	0.925	159.6	0.7797	−1.043	0.826	339.0	0.7907	−0.952	0.737
59.9	0.7731	−1.097	0.894	199.5	0.7822	−1.022	0.802				
79.8	0.7744	−1.086	0.879	239.3	0.7847	−1.002	0.781				
						x_1 = 0.5002					
1.0	0.7773	−1.201	0.913	119.7	0.7853	−1.125	0.830	289.2	0.7959	−1.032	0.745
20.0	0.7786	−1.188	0.898	159.6	0.7879	−1.102	0.807	339.0	0.7988	−1.008	0.727
59.9	0.7814	−1.161	0.869	199.5	0.7904	−1.079	0.786				
79.8	0.7827	−1.149	0.856	239.3	0.7929	−1.058	0.767				
						x_1 = 0.5986					
1.0	0.7845	−1.168	0.898	119.7	0.7925	−1.094	0.816	289.2	0.8029	−0.999	0.731
20.0	0.7858	−1.156	0.883	159.6	0.7950	−1.071	0.793	339.0	0.8058	−0.974	0.712
59.9	0.7885	−1.130	0.854	199.5	0.7975	−1.048	0.772				
79.8	0.7899	−1.118	0.841	239.3	0.7999	−1.026	0.752				
						x_1 = 0.7975					
1.0	0.7964	−0.750	0.890	119.7	0.8044	−0.707	0.807	289.2	0.8148	−0.644	0.719
20.0	0.7977	−0.743	0.876	159.6	0.8070	−0.693	0.783	339.0	0.8177	−0.625	0.698
59.9	0.8004	−0.729	0.847	199.5	0.8095	−0.678	0.762				
79.8	0.8018	−0.722	0.833	239.3	0.8119	−0.663	0.741				
						x_1 = 1.0000					
1.0	0.8059	0.00	0.885	119.7	0.8141	0.00	0.810	289.2	0.8247	0.00	0.731
20.0	0.8073	0.00	0.871	159.6	0.8166	0.00	0.788	339.0	0.8277	0.00	0.713
59.9	0.8100	0.00	0.845	199.5	0.8192	0.00	0.769				
79.8	0.8114	0.00	0.833	239.3	0.8217	0.00	0.751				

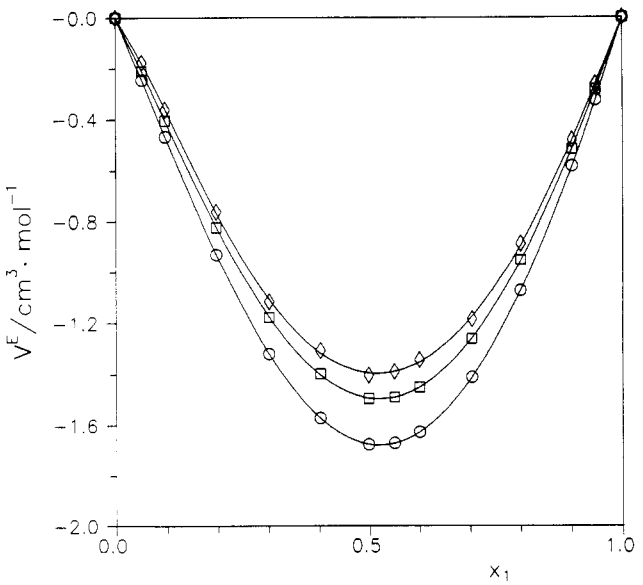

Figure 7. Excess molar volume, V^E, of the system methanol (1) + n-butylamine (2) at 298.15 K: ○, 1.0 bar; □, 199.5 bar; ◇, 339.1 bar; —, eq 8.

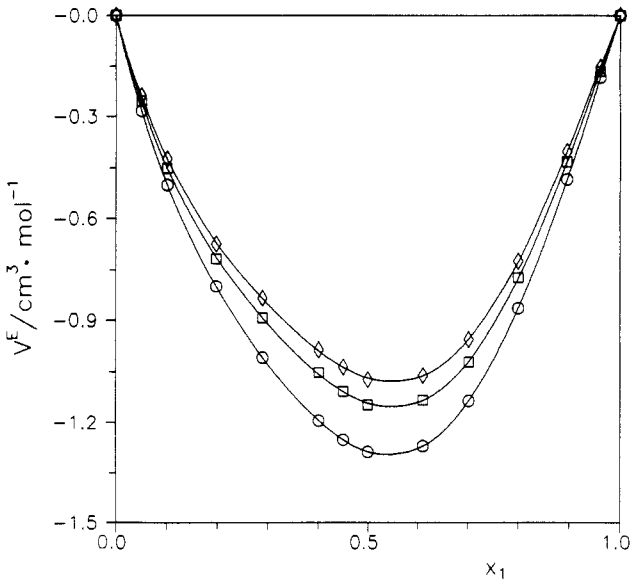

Figure 8. Excess molar volume, V^E, of the system ethanol (1) + n-butylamine (2) at 298.15 K. Symbols as in Figure 7.

by a palmograph, model HM203-6 of Hameg, connected in parallel to the timing circuit.

The lower end of the tube is permanently screwed to the pressure-transmitting device while the upper end is sealed with a plug after having been filled with the liquid under study. Around the viscometer tube circulates water by means of a Haake ultrathermostat which keeps the temperature of the liquid constant to within ±0.01 °C over long periods of time. The compression cell of the viscometer is similar to the one used for the density measurements. A long stainless steel tube (outside diameter 1/8 in.), containing the same hydraulic fluid, is used to connect the dead-weight tester with the compression cell of the viscometer. A schematic view of the experimental setup for the measurement of viscosity is shown in Figure 3. The viscometer was held in a vertical position by means of the two horizontal bars 4 and 6 shown in Figure 3. The sinker returns to its initial position by rotating the viscometer around bar 4. Bar 6 positions the viscometer precisely vertically for the fall of the sinker which in turn triggers the timing circuit.

As already mentioned the viscometer constant, A, is independent of temperature and pressure. It can be deter-

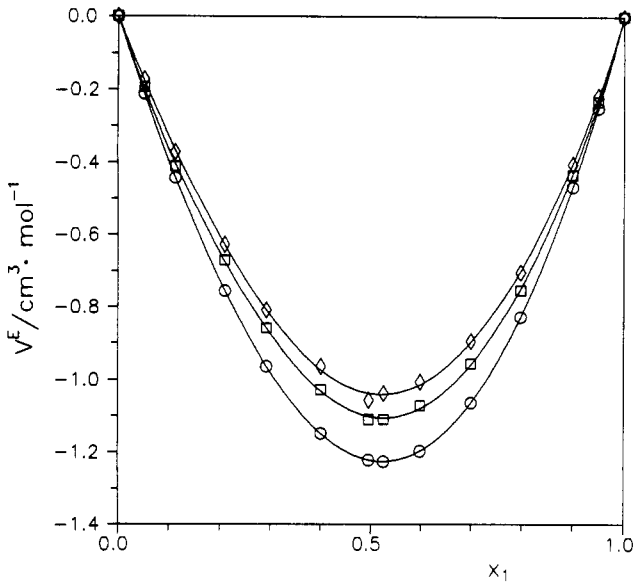

Figure 9. Excess molar volume, V^E, of the system 1-propanol (1) + *n*-butylamine (2) at 298.15 K. Symbols as in Figure 7.

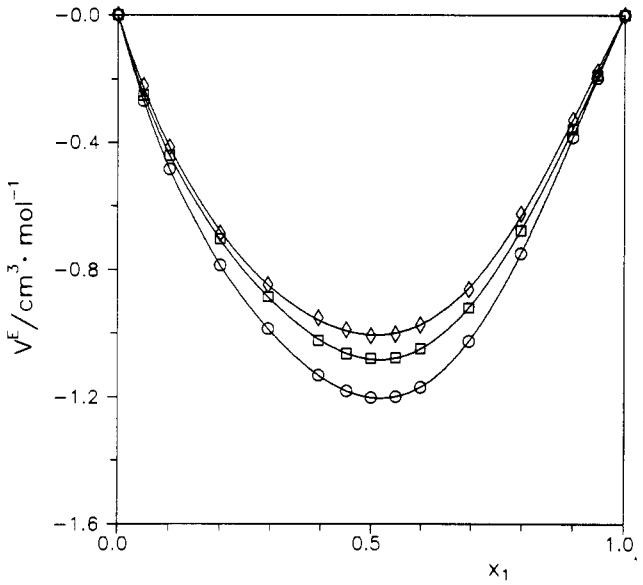

Figure 10. Excess molar volume, V^E, of the system 1-butanol (1) + *n*-butylamine (2) at 298.15 K. Symbols as in Figure 7.

mined, then, by calibration with liquids of known viscosity at atmospheric pressures. Due to the onset of nonlaminar flow A is found to increase slightly with increasing Reynolds number, N_{Re}, at short fall times. This turbulence effect is described by the equation (*8*)

$$A = A_r\left\{1 + \left[\frac{B}{t(1-\rho_L/\rho_S)}\right]\right\} \tag{3}$$

where A_r, B, and N are instrumental constants to be determined. The density of the sinker, ρ_S, at temperature T and pressure P can be calculated from the density ρ_{Sr} at a reference state by the equation

$$\rho_S = \frac{\rho_{Sr}}{[1 + 3\alpha(T-T_r)][1-\beta(P-P_r)]} \tag{4}$$

The density ρ_{Sr} of the sinker at the reference state was determined by weighing it in air and in distilled water, and it was found that ρ_{Sr} = 7.907 49 g·cm^{-3}. With known compressibility of the magnetic material of the sinker, β = 1.95 × 10^{-12} Pa^{-1}, eq 4 may be used to give the density of the sinker at any pressure and at the reference temperature. For

Table VI. Coefficients v_j of Equation 8 and Standard Deviation of Fit σ

P/bar	v_0	v_1	v_2	v_3	v_4	100σ/(cm^3·mol^{-1})
			Methanol (1) + *n*-Butylamine (2)			
1.0	−6.7093	0.5955	1.1312	0.2314	0.0086	0.03
199.5	−5.9889	0.5272	1.0255	0.2637	0.2220	0.23
339.1	−5.5904	0.3772	0.7122	0.6083	0.8422	0.76
			Ethanol (1) + *n*-Butylamine (2)			
1.0	−5.1533	0.9552	0.0135	−1.8519	−0.5392	0.02
199.5	−4.5793	0.9700	−0.0699	−1.8987	−0.4605	0.33
339.1	−4.2811	0.9175	−0.1157	−1.8357	−0.3438	0.30
			1-Propanol (1) + *n*-Butylamine (2)			
1.0	−4.8918	0.4845	0.1409	0.0217	0.0019	0.00
199.5	−4.4146	0.4930	0.4055	−0.0136	−0.6446	0.60
339.1	−4.1584	0.4038	0.4489	0.1891	−0.4705	0.83
			1-Butanol (1) + *n*-Butylamine (2)			
1.0	−4.8038	0.3940	0.1578	−1.6927	−0.1419	0.01
199.5	−4.3260	0.3289	0.3158	−1.4146	−0.6357	0.23
339.1	−4.0202	0.1582	−0.2390	−1.1763	0.2199	0.53

measurements at the referenced state, rearrangement of eq 2 gives

$$A = \frac{t_r(1-\rho_{Lr}/\rho_{Sr})}{\eta_r} \tag{5}$$

Subscript r denotes properties at the reference state. η_r, t_r, and ρ_{Lr} were measured for a number of liquids (reference state, atmospheric pressure and 25 °C), and A was calculated on the basis of eq 5. To these values of A was subsequently applied eq 3, and the instrumental constants A_r, B, and N were then obtained by a least-squares fit. The values thus obtained are A_r = 34.8749 mPa^{-1}, B = 5.2146 s, and N = 1.7002. The resulting calibration curve is shown in Figure 4. The average absolute percent deviation of the fit is 2.069%.

Systematic errors are minimized when calculating at the reference temperature the viscosity ratio, η/η_r, at pressure P and at atmospheric pressure. In this case the working equation is

$$\frac{\eta}{\eta_r} = \frac{t}{t_r}\frac{(1-\rho_L/\rho_S)}{(1-\rho_{Lr}/\rho_{Sr})}\frac{\left\{1+\left[\frac{B}{t(1-\rho_{Lr}/\rho_{Sr})}\right]^N\right\}}{\left\{1+\left[\frac{B}{t(1-\rho_L/\rho_S)}\right]^N\right\}[1-1.5\beta(P-P_r)]} \tag{6}$$

At least eight fall-time measurements were done, and the reported viscosity coefficient is the average of these measurements. From eq 6, for the calculation of viscosity one must know the density of the liquid. Our densitometer can be used for pressures up to 400 bar. In order to estimate the densities at the higher pressures, we have tested the Tait equation of state for a large number of data on pure components and mixtures of the literature as to whether it can reproduce the experimental densities at higher pressures when its parameters are estimated from experimental data at lower pressures (e.g., below 400 bar). This extrapolation was quite satisfactory at pressures as high as 750 bar which cover our pressure range. In Figures 5 and 6 are compared our experimental data with corresponding data from the literature (*8*, *9*) for pure methanol and propanol.

When the temperature and pressure were stable over long periods of time, the measurements were reproducible with a maximum deviation between any two of them of ±0.06%. Taking into account the fluctuations in the pressure during lengthy runs (usually less than 0.03 bar) and the fluctuations

Table VII. Experimental Viscosities for the System Methanol (1) + n-Butylamine (2) at 298.15 K

	η/(mPa·s)										
P/bar	x_1 = 0.000	x_1 = 0.100	x_1 = 0.203	x_1 = 0.299	x_1 = 0.399	x_1 = 0.501	x_1 = 0.598	x_1 = 0.697	x_1 = 0.796	x_1 = 0.900	x_1 = 1.000
1.0	0.468	0.505	0.552	0.599	0.653	0.707	0.747	0.761	0.732	0.650	0.546
44.7	0.484	0.524	0.573	0.623	0.678	0.733	0.772	0.785	0.751	0.666	0.557
94.6	0.502	0.545	0.598	0.650	0.707	0.762	0.800	0.811	0.772	0.685	0.569
144.4	0.520	0.567	0.622	0.676	0.736	0.792	0.829	0.838	0.794	0.704	0.581
194.3	0.538	0.588	0.647	0.703	0.765	0.821	0.857	0.865	0.816	0.723	0.594
244.1	0.556	0.610	0.671	0.730	0.794	0.851	0.886	0.892	0.837	0.742	0.606
293.9	0.574	0.631	0.696	0.757	0.823	0.881	0.915	0.919	0.859	0.761	0.619
343.8	0.592	0.653	0.721	0.784	0.853	0.910	0.944	0.946	0.881	0.781	0.632
393.7	0.610	0.675	0.745	0.811	0.882	0.940	0.973	0.973	0.903	0.800	0.644
518.1	0.656	0.729	0.807	0.879	0.956	1.015	1.045	1.041	0.958	0.848	0.676
717.5	0.729	0.817	0.907	0.989	1.074	1.136	1.162	1.150	1.047	0.926	0.727

Table VIII. Experimental Viscosities for the System Ethanol (1) + n-Butylamine (2) at 298.15 K

	η/(mPa·s)									
P/bar	x_1 = 0.102	x_1 = 0.150	x_1 = 0.295	x_1 = 0.449	x_1 = 0.501	x_1 = 0.595	x_1 = 0.680	x_1 = 0.752	x_1 = 0.897	x_1 = 1.000
1.0	0.514	0.542	0.626	0.749	0.791	0.872	0.931	0.977	1.051	1.087
44.7	0.534	0.565	0.651	0.780	0.823	0.907	0.967	1.013	1.087	1.119
94.6	0.557	0.591	0.679	0.815	0.859	0.948	1.007	1.053	1.127	1.155
144.4	0.581	0.617	0.708	0.849	0.895	0.989	1.048	1.094	1.168	1.192
194.3	0.604	0.643	0.736	0.884	0.932	1.029	1.089	1.134	1.209	1.228
244.1	0.627	0.669	0.764	0.919	0.969	1.070	1.130	1.175	1.251	1.265
293.9	0.650	0.695	0.793	0.955	1.005	1.111	1.171	1.216	1.292	1.302
343.8	0.674	0.722	0.821	0.990	1.042	1.152	1.212	1.257	1.333	1.338
393.7	0.697	0.748	0.850	1.025	1.079	1.193	1.253	1.298	1.375	1.375
518.1	0.756	0.814	0.921	1.114	1.171	1.296	1.356	1.401	1.479	1.468
717.5	0.851	0.920	1.037	1.256	1.320	1.463	1.523	1.567	1.647	1.619

Table IX. Experimental Viscosities for the System 1-Propanol (1) + n-Butylamine (2) at 298.15 K

	η/(mPa·s)									
P/bar	x_1 = 0.100	x_1 = 0.198	x_1 = 0.301	x_1 = 0.417	x_1 = 0.501	x_1 = 0.600	x_1 =0.695	x_1 = 0.786	x_1 = 0.925	x_1 = 1.000
1.0	0.534	0.612	0.711	0.846	0.965	1.117	1.273	1.451	1.760	1.968
44.7	0.555	0.637	0.740	0.882	1.006	1.165	1.328	1.511	1.828	2.039
94.6	0.579	0.665	0.774	0.923	1.053	1.219	1.390	1.579	1.905	2.121
144.4	0.603	0.694	0.807	0.964	1.099	1.273	1.453	1.643	1.983	2.203
194.3	0.627	0.722	0.841	1.005	1.146	1.327	1.515	1.717	2.061	2.285
244.1	0.651	0.750	0.875	1.046	1.193	1.382	1.578	1.786	2.139	2.368
293.9	0.675	0.779	0.908	1.087	1.240	1.437	1.641	1.855	2.217	2.451
343.8	0.699	0.807	0.942	1.129	1.287	1.492	1.704	1.925	2.296	2.534
393.7	0.723	0.836	0.976	1.170	1.334	1.547	1.768	1.994	2.375	2.617
518.1	0.784	0.907	1.061	1.274	1.452	1.685	1.926	2.169	2.573	2.826
717.5	0.881	1.023	1.197	1.442	1.643	1.907	2.183	2.452	2.893	3.165

in temperature (less than 0.01 °C), the viscosity coefficients are estimated to be measured with an accuracy better than ±1% in the range of pressures up to 400 bar. The uncertainty in the density at higher pressures is the main source of increased uncertainty in viscosity data at this range of pressure. In any case, however, the accuracy of the reported data on viscosity at pressures higher than 400 bar is estimated to be better than ±2.5%.

Results

For each binary mixture we have conducted measurements of density at 12 intermediate compositions (plus the two pure components) and at 30 pressures, from atmospheric to 340 bar, for each composition. From these data on density one can calculate the isothermal compressibility, β_T, of the mixture and the excess volume, V^E. The latter quantity for a mixture of components 1 and 2 is defined as

$$V^E = V - x_1V_1 - x_2V_2 = x_1M_1\left(\frac{1}{\rho} - \frac{1}{\rho_1}\right) + x_2M_2\left(\frac{1}{\rho} - \frac{1}{\rho_2}\right) \quad (7)$$

where M_i is the molar mass of component i.

In Tables II–V are reported the experimental densities of the four binary mixtures at 25 °C along with the calculated excess volume and the isothermal compressibility. Experimental data are reported for five intermediate compositions. At each of these compositions are reported data at only 10 pressures. The full tables with data at all pressures and compositions are available upon request from the authors.

In Figures 7–10 are shown the experimental excess volumes at three pressures for the four binary mixtures. The solid lines were calculated by fitting to the experimental data a Redlich–Kister-type equation

$$V^E/(\mathrm{cm^3 \cdot mol^{-1}}) = x_1x_2\sum_{j=0}^{n} v_j(1 - 2x_1)^j \quad (8)$$

Coefficients v along with the standard deviation of fit are reported in Table VI.

For each binary system we have conducted viscosity measurements at 12 intermediate compositions (plus 2 for the pure components) and at 16 pressures, from atmospheric to 720 bar, for each composition. In Tables VII–X are reported the experimental viscosities for 9 intermediate compositions of the mixture at 11 applied pressures. From these data on viscosities one can calculate the viscosity deviation, $\Delta\eta$, of the mixture defined by

$$\Delta\eta = \eta - x_1\eta_1 - x_2\eta_2 \quad (9)$$

In Figures 11–14 are shown the experimental viscosity deviations of the four binary mixtures at four external pressures. The solid lines were calculated by fitting to the

Table X. Experimental Viscosities for the System 1-Butanol (1) + n-Butylamine (2) at 298.15 K

	η/(mPa·s)									
P/bar	x_1 = 0.099	x_1 = 0.195	x_1 = 0.294	x_1 = 0.401	x_1 = 0.493	x_1 = 0.600	x_1 = 0.695	x_1 = 0.800	x_1 = 0.893	x_1 = 1.000
1.0	0.553	0.663	0.794	0.951	1.101	1.312	1.531	1.818	2.131	2.578
44.7	0.575	0.692	0.830	0.994	1.150	1.369	1.599	1.902	2.231	2.690
94.6	0.600	0.726	0.871	1.042	1.205	1.433	1.676	1.998	2.346	2.819
144.4	0.625	0.759	0.912	1.090	1.260	1.498	1.754	2.095	2.462	2.948
194.3	0.650	0.792	0.952	1.139	1.315	1.563	1.831	2.192	2.577	3.077
244.1	0.675	0.826	0.993	1.187	1.371	1.628	1.909	2.290	2.693	3.207
293.9	0.700	0.859	1.034	1.236	1.426	1.693	1.987	2.388	2.809	3.338
343.8	0.725	0.893	1.076	1.285	1.482	1.759	2.066	2.486	2.926	3.468
393.7	0.751	0.927	1.117	1.334	1.538	1.824	2.144	2.584	3.043	3.600
518.1	0.814	1.011	1.220	1.456	1.678	1.989	2.341	2.830	3.337	3.929
717.5	0.915	1.147	1.386	1.654	1.904	2.255	2.660	3.230	3.812	

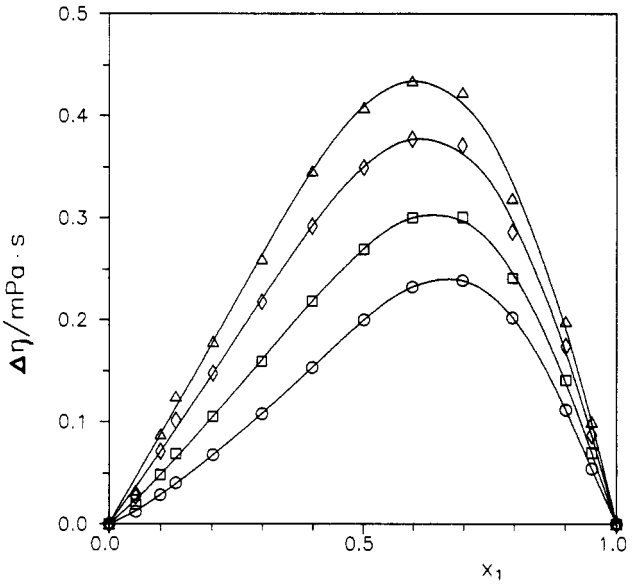

Figure 11. Excess dynamic viscosity, η^E, of the system methanol (1) + n-butylamine (2) at 298.15 K: ○, 1.0 bar; □, 244.1 bar; ◇, 518.1 bar; △, 717.5 bar; —, eq 10.

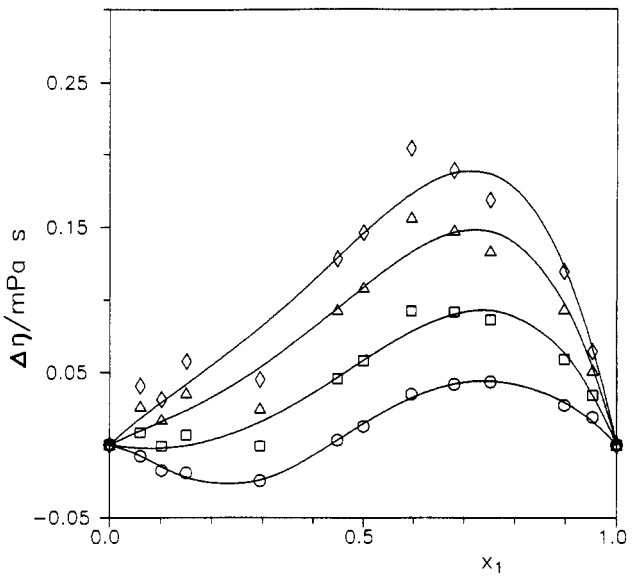

Figure 12. Excess dynamic viscosity, η^E, of the system ethanol (1) + n-butylamine (2) at 298.15 K. Symbols as in Figure 11.

experimental data the Redlich–Kister-type equation

$$\Delta\eta/(\text{Pa·s}) = x_1x_2\sum_{j=0}^{n} h_j(1-2x_1)^j \qquad (10)$$

Coefficients h_j along with the standard deviation of fit are reported in Table XI.

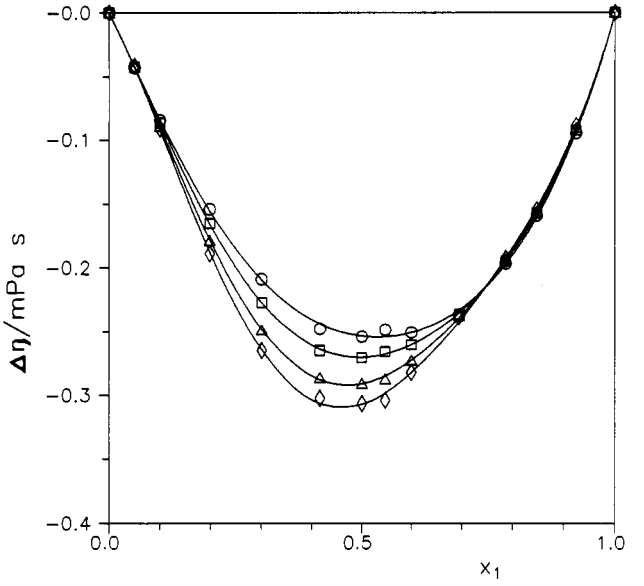

Figure 13. Excess dynamic viscosity, η^E, of the system 1-propanol (1) + n-butylamine (2) at 298.15 K. Symbols as in Figure 11.

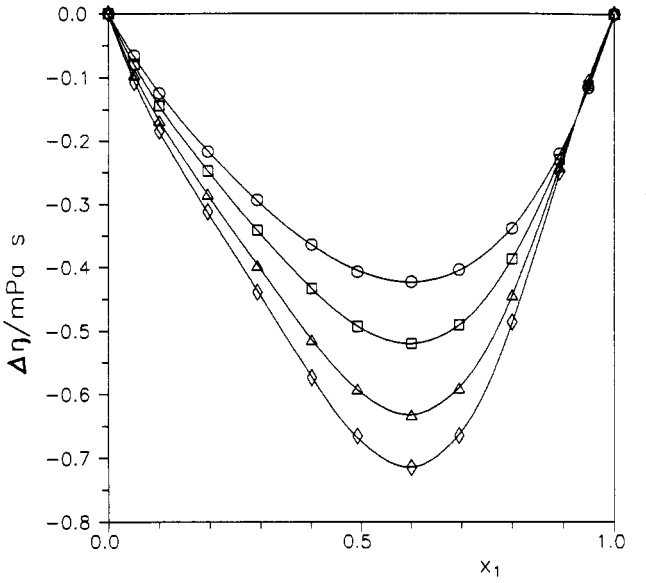

Figure 14. Excess dynamic viscosity, η^E, of the system 1-butanol (1) + n-butylamine (2) at 298.15 K. Symbols as in Figure 11.

Discussion

Prior to the discussion of the behavior of the binary mixtures it is worth comparing the properties of the pure components. From Tables II–V and VII–X one can see that butylamine and methanol have similar isothermal compressibilities and

Table XI. Coefficients h_j of Equation 10 and Standard Deviation of Fit σ

P/bar	h_0	h_1	h_2	h_3	h_4	100σ/(mPa·s)
			Methanol (1) + *n*-Butylamine (2)			
1.0	0.7961	−0.8392	0.2571	0.4098	−0.4329	0.04
244.1	1.0776	−0.8618	0.1161	0.3704	−0.2686	0.32
518.1	1.3978	−0.8896	−0.0464	0.3291	−0.0768	0.65
717.5	1.6329	−0.9116	−0.1669	0.3006	0.0659	0.90
			Ethanol (1) + *n*-Butylamine (2)			
1.0	0.0587	−0.4285	−0.1053	0.1975	0.2212	0.23
244.1	0.2330	−0.4451	0.1573			0.85
518.1	0.4354	−0.5530	0.2907			1.41
717.5	0.5832	−0.6327	0.3880			1.82
			1-Propanol (1) + *n*-Butylamine (2)			
1.0	−1.0139	0.0975	−0.2251	0.2171	0.0892	0.28
244.1	−1.0824	−0.0170	−0.0806	0.3464	0.0282	0.09
518.1	−1.1652	−0.1468	0.0829	0.4926	−0.0384	0.12
717.5	−1.2286	−0.2424	0.2045	0.5990	−0.0888	0.28
			1-Butanol (1) + *n*-Butylamine (2)			
1.0	−1.6277	0.6240	−0.2577	−0.0449	−0.1623	0.15
244.1	−1.9805	0.9439	−0.0305	−0.6841	−0.0346	0.03
518.1	−2.3895	1.3078	0.2257	−1.4097	0.1155	0.10
717.5	−2.6942	1.5752	0.4128	−1.9447	0.2294	0.21

viscosities. The compressibilities of the other alkanols are smaller and decrease as the chain length of the alkanol molecule increases. The increase, however, of the viscosity with the chain length is much more pronounced; the viscosity of butanol is almost an order of magnitude larger than the viscosity of butylamine although their molecular sizes are similar. Alkanol molecules self-associate strongly (OH···OH interaction) while the amine molecules rather marginally[10] and this has a remarkable influence on the studied properties.

As is shown in Figures 7–10, all binary systems studied exhibit relatively large negative excess volumes which persist over the pressure range studied here. V^E is especially large (negative) in the mixture with methanol and decreases as the chain length of the alkanol increases. The transition from methanol to ethanol is much steeper compared to the transition from ethanol to butanol. This is certainly indicative of the relative strength of the specific interactions between the hydroxyl and the amine groups in the four mixtures. We are conducting at present a parallel systematic study of the heats of mixing in this type of system, and the complete results will be published in a forthcoming paper. It is however worth mentioning here that the largest negative heats of mixing measured at 25 °C are −3815, −2915, −2870, and −2705 J·mol^{-1} for the mixtures of *n*-butylamine with methanol, ethanol, 1-propanol, and 1-butanol, respectively. The picture emerging from these values is similar to that of the excess volumes and indicates that the hydrogen bonding of butylamine with the methanol molecule is much stronger than with the other lower alkanols.

The large negative excess volume in the mixture with methanol indicates that a most efficient packing of the molecules occurs in this mixture. Aside from the strength of the OH···NH_2 interaction (compared to the strength of the OH···OH, and NH_2···NH_2 interactions), this efficiency arises also from the relative sizes of the methanol and butylamine molecules.

An inspection of Figures 11–14 indicates that the strength of the intermolecular hydrogen bonding is not the only factor influencing the viscosity deviation of liquid mixtures. The molecular sizes and shapes of the components are equally (if not more) important factors. It is doubtless however that the strength of hydrogen bonding between the methanol and butylamine molecules is the main factor for the occurrence of the not too common positive excess viscosities in their mixture. Although one may question the physical meaning of the viscosity deviation (often referred to as excess viscosity), Figures 11–14 indicate that, as far as this quantity is concerned, the transition from the mixture with methanol to that with butanol is much more clear compared to the behavior of excess volumes. There is a smooth and pronounced decrease of the maximum viscosity deviation when going from the mixture with methanol to that with butanol. The figures also show that, as the pressure increases, the viscosity deviation behaves much differently from the excess volumes. At least over the pressure range studied here, the viscosity deviation in the mixtures with methanol and ethanol increases as the pressure increases while in the other two mixtures the effect of pressure is the reverse.

Theoretical developments could certainly assist in providing more solid interpretation of the thermophysical behavior of our systems. As already mentioned, the thrust for the present viscosity measurements has originated from the need for accurate estimations of the limiting ratio of viscosity over pressure as the pressure tends to zero. Work is in progress in our laboratory toward the development of a semitheoretical model for the viscosity of multicomponent liquid mixtures along the lines of our previous work (*1*, *10*).

Literature Cited

(1) Mamagakis, N.; Panayiotou, C. *Z. Phys. Chem. N.E.* **1989**, *162*, 57.
(2) Panayiotou, C. *Pure Appl. Chem.* **1989**, *61*, 1453.
(3) Kell, S. G.; Whalley, E. *J. Chem. Phys.* **1975**, *62*, 3496.
(4) Machado, J. R. S.; Street, W. B. *J. Chem. Eng. Data* **1983**, *28*, 218.
(5) Isdale, J. D.; Spence, C. M. *NEL Rep. (G.B.)* **1975**, *592*, (June).
(6) Dymond, J. H.; Robertson, J.; Isdale, J. D. *Int. J. Thermophys.* **1981**, *2*, 133.
(7) Dymond, J. H.; Glen, N. F.; Isdale, J. D. *Int. J. Thermophys.* **1985**, *6*, 233.
(8) Isdale, J. D.; Easteal, A. J.; Woolf, L. A. *Int. J. Thermophys.* **1985**, *6*, 439.
(9) Tanaka, Y.; Matsuda, Y.; Fujiwara, H.; Kubota, H.; Makita, T. *Int. J. Thermophys.* **1987**, *8*, 147.
(10) Panayiotou, C. *J. Solution Chem.* **1991**, *20*, 97.
(11) Riddick, J. A.; Bunger, W. B., *Organic Solvents. Techniques of Chemistry*; Wiley-Interscience: New York, 1970; Vol. II.
(12) Wei, I. Ph.D. Thesis, Rice University, Houston, TX, 1984.
(13) Aithal, U. S.; Aminabhavi, T. M.; Shukla, S. S. *J. Chem. Eng. Data* **1990**, *35*, 298.
(14) Mumford, S. A.; Philips, J. W. C. *J. Chem. Soc.* **1950**, 75.
(15) Letcher, T. M.; Bayles, J. W. *J. Chem. Eng. Data* **1971**, *16*, 266.
(16) Reid, R. C.; Prausnitz, J. M.; Sherwood, T. K. *The Properties of Gases and Liquids*, 3rd ed.; McGraw Hill: New York, 1977.

Received for review December 15, 1992. Accepted March 5, 1993.